2011 50th IEEE Conference on Decision and Control and
European Control Conference (CDC-ECC)
Orlando, FL, USA, December 12-15, 2011

Output Maneuvering Control Scheme for a Car-like Mobile Robot

H. Rodríguez-Cortés, M. Velasco-Villa

Abstract— **In this paper, we propose an output maneuvering nonlinear controller for the car-like mobile robot. The control approach is based on a combination of the input-output feedback linearization control technique and the output maneuvering control approach introduced in [1]. It is shown that the closed–loop system is asymptotically stable and the path following error converges asymptotically to zero when an accurate car-like mobile robot localization system is available, and it is shown that when the car-like mobile robot position is not accurately estimated (for instance, under the influence of noise measurements) the closed–loop dynamics remains ultimately bounded. Numerical simulations are performed to show the overall performance of the proposed scheme in both cases.**

I. Introduction

In recent years, autonomous robots have demonstrated their usefulness in different applications ranging from very expensive military applications to relatively cheap and mass produced home applications. To extend the civilian potential uses of autonomous robots, for instance in surveillance applications, the capability to plan paths and to follow them accurately, specially when non expensive position sensors are used, is of great importance.

Mobile robot localization is a fundamental problem in mobile robot applications, the many partial solutions can roughly be categorized into two groups: relative and absolute position measurements, [2]. For indoor applications both groups of solutions, such as odometry, inertial navigation, active beacons and landmark navigation, provide relatively accurate position measurements mainly because the environment is in some sense controlled. For instance, the terrain can be carefully selected to reduce slipping for a successful odometry application. However, for outdoor applications the mobile robot localization problem has not many successful solutions; in this case it is more difficult to achieve a tight control of the environment. Some promising solutions for mobile robot localization have been obtained by means of global positioning systems (GPS), inertial measurement units (IMU) and compass sensors (CS). These measurements are fused to provide an estimation of the position of the mobile robot with respect to an inertial frame. However, due to the deliberated small errors in timing and satellite position of the GPS, there is a bias error associated to the GPS, IMU and CS based position measurement.

Current position measurement systems available in the civil market, based on GPS, IMU and MC, have an associated bias of approximately 10 m virtually unchanging over a long period of time and a random error in the range of $2-3$ m. A successful control strategy to perform trajectory tracking or path following must be robust against this position measurement errors. For instance in [3] a successful path following scheme for miniature air vehicles is achieved in the presence of this kind of localization errors. Even though, the closed–loop stability analysis in the presence of localization errors is not performed, the experimental results show that the controller is able to handle such localization errors.

Several approaches have been proposed for car-like mobile robots trajectory tracking; [4], [5] and path following; [6], [7]. See [8] for a solution of both problems: trajectory tracking and path following in the case of parametric modeling uncertainty. In [9], it is introduced a model of the car-like mobile robot in the presence of skidding and slipping effects, then in [10] a robust control scheme against the skidding and slipping effects based on a backstepping technique is presented. Experimental results are performed using a high grade GPS to measure position and velocity.

Control strategies for trajectory tracking have the objective of driving the mobile robot to a certain point of the trajectory at a particular time. Hence, trajectory tracking control strategies rely on precise mobile robot localization algorithms. The trajectory tracking error will increase without taking into account the actual position of the mobile robot. On the other hand, control strategies for path following have the primary objective of driving the mobile robot to the path unrelated to time and as a secondary objective to satisfy an additional dynamic specification, for instance the speed along the path.

Another topic to be considered in mobile robot applications is the path generation problem. The path generation algorithm must produces feasible trajectories that satisfy exact timing or path length constraints. In [11] is proposed a trajectory generation algorithm that decomposes the trajectory generation problem into two steps: a way point planning step, where the straight line paths are not time- parameterized, and a time-parameterized trajectory generation step to smooth the way point paths into dynamically feasible trajectories. In [12] its is proposed a new path primitive called η^3-spline which permits the interpolation of an arbitrary sequence of points with associated arbitrary tangent directions, curvatures, and curvature derivatives. In [13] it is presented a suboptimal 2-D path satisfying initial and terminal conditions, specified in terms of position and heading angle. An empirical extension is presented for the 3-D case. A common issue in this non exhaustive review of path generation algorithms is that they rely on an accurate mobile robot localization. In this work we solve the path generation problem by means of a special

H. Rodríguez-Cortés and M. Velasco-Villa are with CINVESTAV-IPN, Departamento de Ingeniería Eléctrica, Sección de Mecatrónica, Av. IPN 2508, Col. San Pedro Zacatenco, CP 07360, México D.F., México. {hrodriguez,velasco}@cinvestav.mx

planar curve that produces a path that allows to survey two supposed hot points, the Cassini's oval, [14].

In this paper, we propose an output maneuvering nonlinear controller for the car-like mobile robot. The control approach is based on a combination of the input-output feedback linearization ([15], [16], [17]) control technique and the output maneuvering control approach introduced in [1]. It is shown that the closed–loop system is asymptotically stable and the path following error converges asymptotically to zero when an accurate car-like mobile robot localization system is available, and it is shown that when the car-like mobile robot position is not accurately estimated the closed–loop dynamics remains ultimately bounded and the path following error converges to a neighborhood of zero. Numerical simulations are carried out to show the overall performance of the proposed scheme in both cases.

The rest of the paper is organized as follows. In Section II we describe the kinematic model of the car–like mobile robot and formulate the path following control problem that we address. Section III presents a nonlinear control law to solve the path following problem and discusses the stability of the resulting closed–loop system in both cases: accurate and non accurate car-like mobile robot localization. In Section IV we illustrate the main features of the proposed control scheme through numerical simulations. Finally, in Section V the paper concludes with remarks about the proposed results and recommendations for further research.

II. Kinematic model of the car-like mobile robot

The wheeled mobile robot considered in this work is of a $(1,1)$–type ([18], [19]), it possesses one degree of mobility and one degree of steerability, known as the car-like mobile robot. This wheeled mobile robot has front parallel steerable wheels and fixed parallel rear wheels, see figure II.

Let $\{X^i, Y^i\}$ denote a right- hand inertial frame, and let $\{X^b, Y^b\}$ denote a right-hand frame fixed to the car-like mobile robot at the reference point P. In Figure II,

$$X = \begin{bmatrix} x & y \end{bmatrix}^\top \tag{1}$$

denotes the reference point P inertial coordinates, ζ denotes the front wheel steering angle, ψ denotes the car-like mobile robot orientation and ℓ denotes the car-like mobile robot wheelbase. Summarizing, the car-like mobile robot posture is defined as $q = \begin{bmatrix} x & y & \psi \end{bmatrix}^\top$

Under the kinematic constraints of non slipping and pure rolling condition the posture kinematic model for the car-like mobile robot is described by the following set of differential equations

$$\begin{aligned} \dot{x} &= V\cos(\psi) \\ \dot{y} &= V\sin(\psi) \\ \dot{\psi} &= \tfrac{V}{\ell}\tan(\zeta) \end{aligned} \tag{2}$$

where V denotes the velocity of the car-like mobile robot.

The path following control problem can be stated as in [1]. Given a desired parametrized path

$$Y_d = \left\{ y \in \mathbb{R}^m \,:\, \exists\, \theta \in \mathbb{R} \text{ such that } y = y_d(\theta) \right\} \tag{3}$$

where $y_d(\theta)$ is continuously parametrized by the path, the output maneuvering problem with speed assignment comprises two tasks:

- *Geometric task*. Force the output y to converge to the desired path $y_d(\theta)$,
$$\lim_{t\to\infty} |y(t) - y_d(\theta(t))| = 0$$
- *Speed assignment*. Force the path speed to converge to a desired speed v_s
$$\lim_{t\to\infty} |\dot{\theta}(t) - v_s(t)| = 0$$

Hence, we define:

Control objective. *Let $X_d(\theta) \in \mathbb{R}^2$ be a desired path for the car-like mobile robot position parameterized by $\theta \in \mathbb{R}$ and $v_s \in \mathbb{R}$ a desired speed assignment. Assume that $X_d(\theta)$ is smooth with respect to θ and its first two derivatives are bounded. Design a control law such that all the closed–loop signals are bounded, the car-like mobile robot position converges and remains in the desired path. Moreover, in the presence of mobile robot localization errors the car-like mobile robot position remains inside a tube centered at the desired path.*

In [1] a solution for the robust output maneuvering problem is proposed for systems in strict feedback form of vector relative degree n

$$\begin{aligned} \dot{x}_1 &= G_1(x_1)x_2 + f_1(x_1) + W(x_1)\delta_1(t) \\ \dot{x}_2 &= G_2(x_1,x_2)x_3 + f_1(x_1,x_2) + W(x_1,x_2)\delta_2(t) \\ &\vdots \\ \dot{x}_n &= G_n(x_1,\cdots,x_{n-1})u + f(x_1,\cdots,x_{n-1}) \\ &\quad + W_n(x_1\cdots x_{n-1})\delta_n(t) \\ y &= h(x_1) \end{aligned}$$

where $x_i \in \mathbb{R}^m$, $i = 1,\cdots,n$ are the state, $y \in \mathbb{R}^m$ is the output , $u \in \mathbb{R}^m$ is the control, and $\delta_i(t)$ are unknown

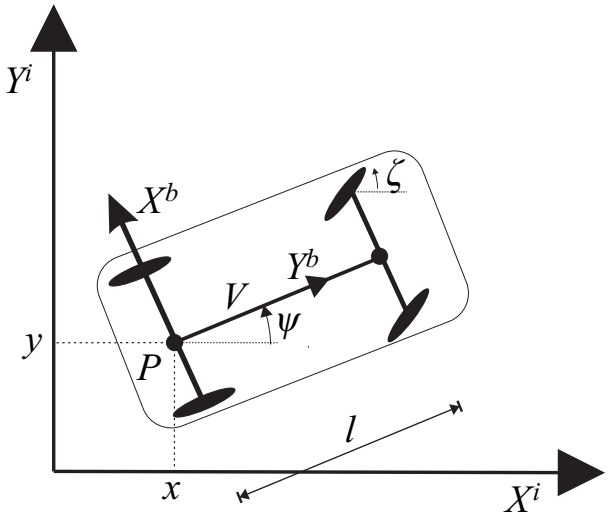

Fig. 1. Car-like Mobile Robot

bounded disturbances. The matrices G_i, f_i and W_i are smooth with G_i and $\frac{\partial h}{\partial x_1}$ invertible. Note that the control problem addressed in this work is slightly different as the disturbance appears through the output of the system.

III. Path following control scheme

In this Section we show that a solution to the control objective can be obtained combining the input-output feedback linearization control technique [20] and the output maneuvering control technique introduced in [1]. To begin with, we consider a dynamic extension to the car-like mobile robot kinematic model (2) and $\tan(\zeta)$ as the second control signal. Under these conditions,

$$\begin{aligned} \dot{x} &= V\cos(\psi) \\ \dot{y} &= V\sin(\psi) \\ \dot{\psi} &= \tfrac{V}{\ell}u_2 \\ \dot{V} &= u_1 \end{aligned} \tag{4}$$

Let us define the path error equation as follows

$$E_1 = X - X_d(\theta) \tag{5}$$

where

$$X_d = \left[\begin{array}{cc} x_d(\theta) & y_d(\theta) \end{array}\right]^\top$$

Straightforward computations show that

$$E_2 = \dot{E}_1 = \dot{X} - \frac{\partial X_d}{\partial \theta}(v_s - \omega_s) \tag{6}$$

where we have considered

$$\dot{\theta} = v_s - \omega_s$$

with ω_s the virtual control law to achieve the speed assignment and v_s the desired path speed. In this paper, v_s takes a constant value. Due to the dynamic extension the control signals do not appear in (6). Taking the time derivative of E_2 we obtain

$$\dot{E}_2 = M(\psi, V)U - F(\theta)(v_s - \omega_s)^2 + G(\theta)\dot{\omega}_s$$

where

$$M(\psi,V) = \left[\begin{array}{cc} \cos(\psi) & -\frac{V^2}{\ell}\sin(\psi) \\ \sin(\psi) & \frac{V^2}{\ell}\cos(\psi) \end{array}\right],\ U = \left[\begin{array}{c} u_1 \\ u_2 \end{array}\right]$$

$$G(\theta) = \left[\begin{array}{c} \frac{\partial x_d}{\partial \theta} \\ \frac{\partial y_d}{\partial \theta} \end{array}\right],\ F(\theta) = \left[\begin{array}{c} \frac{\partial^2 x_d}{\partial \theta^2} \\ \frac{\partial^2 y_d}{\partial \theta^2} \end{array}\right]$$

Defining

$$U = M(\psi,V)^{-1}\left[-K_D E_2 - K_P E_1 + F(\theta)(v_s - \omega_s)^2\right] \tag{7}$$

where K_D and K_P are positive definite matrices, the closed–loop system (4)-(7) reads as

$$\dot{\chi} = A\chi + B\dot{\omega}_s \tag{8}$$

where

$$A = \left[\begin{array}{cc} 0_2 & I_2 \\ -K_D & -K_P \end{array}\right],\ B = \left[\begin{array}{c} 0_1 \\ G(\theta) \end{array}\right],\ \chi = \left[\begin{array}{c} E_1 \\ E_2 \end{array}\right]$$

with 0_2 and I_2 the zero matrix and the identity matrix of dimension 2×2 and 0_1 a zero vector of dimension 2×1.

Note that the closed–loop system in (8) is a linear system in $\chi = \left[\begin{array}{cc} E_1^\top & E_2^\top \end{array}\right]^\top$ perturbed by a term that depends on the parameterization variable of the path and the virtual control related to the speed assignment task. In order to accomplish the control objective we would like to be able to relate the virtual control law ω_s with the distance to the desired path.

Following the work of [1], we consider the following Lyapunov function

$$\mathcal{V} = \frac{1}{2}\chi^\top P\chi + \frac{1}{2}\omega_s^2 \tag{9}$$

with $\chi = \left[\begin{array}{cc} E_1^\top & E_2^\top \end{array}\right]^\top$. The time derivative of the Lyapunov function along the trajectories of (8) gives

$$\dot{\mathcal{V}} = \chi^\top\left(PA + A^\top P\right)\chi + \left(\chi^\top PB + \omega_s\right)\dot{\omega}_s$$

By selecting the gain matrices K_D and K_P in such a way that the matrix A is a Hurtwitz matrix, and by defining $\dot{\omega}_s$ as follows

$$\dot{\omega}_s = -\gamma\left(\omega_s + B^\top P\chi\right) \tag{10}$$

we obtain

$$\dot{\mathcal{V}} = -\frac{1}{2}\chi^\top Q\chi - \gamma\left(\chi^\top PB + \omega_s\right)^2 \tag{11}$$

for a positive definite matrix Q. Hence, we have

Proposition 1: Assume that the desired path $X_d(\theta)$ is smooth, with respect to θ, and its derivatives are bounded. Assume that the car-like mobile robot position X is accurately measured or estimated. Consider the car-like mobile robot kinematic extended model (4) in closed–loop with the control law defined by (7)-(10). Then, for any positive constant γ and any desired constant speed v_s, the equilibrium

$$\chi = 0, \quad \dot{\theta} = v_s \tag{12}$$

is asymptotically stable.

Proof 2: Straightforward computations shows that the closed–loop system (4)-(7)-(10) is described by the following equations

$$\begin{aligned} \dot{\chi} &= A\chi - B\gamma\left(\omega_s + B^\top P\chi\right) \\ \dot{\theta} - v_s &= -\omega_s \\ \dot{\omega}_s &= -\gamma\left(\omega_s + B^\top P\chi\right) \end{aligned} \tag{13}$$

Note now that the Lyapunov function (9) is positive definite radially unbounded and has a unique minimum at $\chi = 0$ and $\omega_s = 0$. In addition, from (11) we conclude that the closed–loop trajectories converge to the largest invariant set contained in

$$\mathcal{D}=\left\{\chi\in\mathbb{R}^2,\omega_s\in\mathbb{R}|\frac{1}{2}\chi^\top Q\chi+\gamma\left(\chi^\top PB+\omega_s\right)^2=0\right\} \tag{14}$$

Finally, it is easy to verify that the largest invariant set of the closed-loop system is compatible with (12). This concludes the proof.

Consider now the case with mobile robot localization errors. In this case the position measurement has a bounded but unknown component $\delta_P(t)$, that is

$$X_m = X+\delta_P(t) \tag{15}$$

with $|\delta_P(t)|\leq\kappa_\delta$. Fortunately, the velocity error estimated from the combination of GPS, IMU and MC is not obtained as $\dot{\delta}_P(t)$. In fact, the velocity error is significantly smaller than the position error, we denote this by $\delta_V(t)$. Since in general it is obtained a good estimation of this signal, we assume in this work that $\delta_V\approx 0$.

Note now that replacing the measured car-like mobile robot position (15) in the feedback control law (7)–(10), we obtain

$$\begin{aligned} U &= M(\psi,V)^{-1}\left[-K_DE_2-K_PE_1+K_P\delta_P(t)\right.\\ &\quad \left.+F(\theta)(v_s-\omega_s)^2\right]\\ \dot{\omega}_s &= -\gamma\left[\omega_s+B^\top P\chi+G^\top P_{12}\delta_P(t)\right] \end{aligned} \tag{16}$$

where we have taken into account that

$$P=\left[\begin{array}{cc} P_{11} & P_{12}\\ P_{12} & P_{22}\end{array}\right]$$

The time derivative of the Lyapunov function (9) along the trajectories of the closed–loop dynamics (4)–(16) reads as

$$\begin{aligned}\dot{\mathcal{V}} &= -\chi^\top Q\chi-\gamma\left(\chi^\top PB+\omega_s\right)^2\\ &\quad +\chi^\top P\bar{K}_P\delta_P(t)+\gamma\left(\chi^\top PB+\omega_s\right)G^\top P_{12}\delta_P(t)\end{aligned}$$

where

$$\bar{K}_P=\left[\begin{array}{c}0_2\\ K_P\end{array}\right]$$

Upper bounding the time derivative of the Lyapunov function we have

$$\begin{aligned}\dot{\mathcal{V}} &\leq -\|\chi\|^2-\gamma\|z\|^2+\|P\|\|K_P\|\kappa_\delta\|\chi\|\\ &\quad +\gamma\kappa_G\|P_{12}\|\kappa_\delta\|z\|\end{aligned}$$

where we have defined $z=\chi^\top PB+\omega_s$, $\|G\|\leq\kappa_G$ and considered $Q=I_2$. For $0<\sigma_i<1$, $i=1,2$ we have

$$\dot{\mathcal{V}}\leq-(1-\sigma_1)\|\chi\|^2-(1-\sigma_2)\|z\|^2,\ \ \forall$$

$$\|\chi\|\geq\frac{\|P\|\|K_P\|\kappa_\delta}{\sigma_1},\ \|z\|\geq\frac{\gamma\kappa_G\kappa_\delta\|P_{12}\|}{\sigma_2}$$

Hence, we have

Proposition 3: Assume that the desired path $X_d(\theta)$ is smooth, with respect to θ, and its derivatives are bounded. Assume that the car-like mobile robot position X is measured from (15) . Consider the car-like mobile robot kinematic extended model (4) in closed–loop with the control law defined by (7)-(10). Then, for any positive constant γ and any desired constant speed v_s, the trajectories of the closed–loop system are uniformly ultimately bounded.

Proof 4: The results follows form the previous computations and the results on stability of systems perturbed by non vanishing perturbations [21].

IV. Numerical simulations

We performed numerical simulation to evaluate the overall performance of the proposed control scheme. We consider as a desired path a Cassini's oval, this curve was selected because generates a path that gives a possible solution to the hypothetical problem of surveying two points, located at curve's focus. The desired Cartesian coordinates parameterized by θ are given by [14]

$$X_d=\sqrt{a^2\cos(2\theta)+\sqrt{b^4-\left(a^2\sin(2\theta)\right)^2}}\left[\begin{array}{c}\cos(\theta)\\ \sin(\theta)\end{array}\right]$$

with a, b constants that define the final shape of the oval, we consider $b=1.5a$. As we expect to test the proposed controller experimentally on a soccer field, we take $a=40$ m.

We consider $K_P=\text{diag}\{k_p,k_p\}$ and $K_D=\text{diag}\{k_d,k_d\}$, consequently

$$\begin{aligned}P_{11} &= \text{any positive definite matrix}\\ P_{12} &= \tfrac{1}{2}K_D^{-1}\\ P_{22} &= \tfrac{1}{2}\left(K_P^{-1}+K_D^{-1}K_P^{-1}\right)\end{aligned}$$

Note that P_{11} is not necessary for control implementation. The controller parameters are summarized in the Table I and the initial conditions in all simulations are summarized in Table II. The car-like mobile robot wheelbase is $\ell=0.3$ m.

TABLE I
CONTROLLER PARAMETERS

k_p	k_d	γ	v_s
6	8	5	0.5

TABLE II
INITIAL CONDITIONS

$x(0)$	$y(0)$	$V(0)$
30	-10	0.5
$\psi(0)$	$\theta(0)$	$\omega_s(0)$
$\pi/4$	0	0

Figure 2 shows the path followed by the car-like mobile robot in the case of trivial localization errors. As it can be observed the car-like mobile robot follows precisely the desired path as predicted by the theoretical computations. The path error signals are shown in Figure 3.

The time history of the control signals is shown in Figure 4. As it can be observed the initial conditions are not close to the desired path this produces high control signals at the beginning of the numerical simulations. We have saturated both control signals.

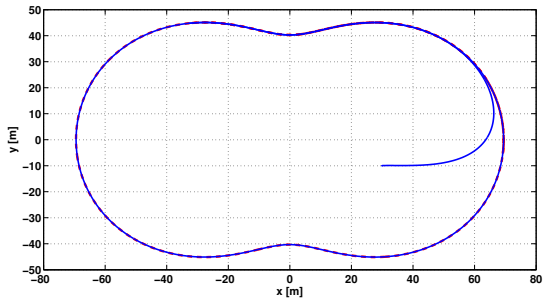

Fig. 2. Simulation results of the path following controller in the idea case. Desired path (dashed line), mobile robot path (continuous line)

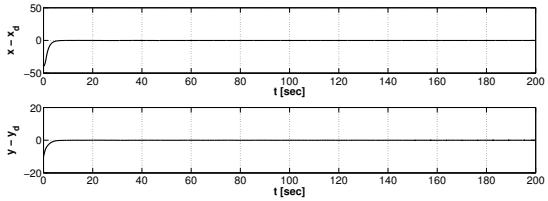

Fig. 3. Path following errors. (top) $x - x_d(\theta)$, (bottom) $y - y_d(\theta)$.

Figure 5 shows the remaining closed–loop system states, that is, the car-like mobile robot velocity and yaw angle. As it can be observed both signals remain bounded.

Finally, in Figure 6 we show the time evolution of the path parameter θ, which as it can be observed has a behavior similar to time, and the evolution of the speed controller ω_s which remains bounded and converges to zero. Note that the convergence of ω_s is quite slow.

We consider now the case of non zero localization errors with the following model for the position error measurement

$$\delta_P(t) = \Delta_1 + \Delta_2 \tag{17}$$

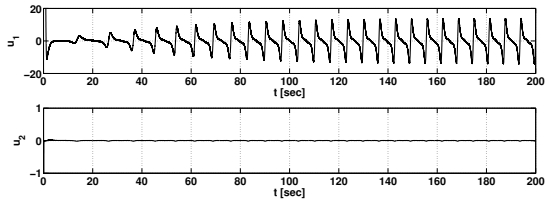

Fig. 4. Control signals. (top) u_1, (bottom) u_2.

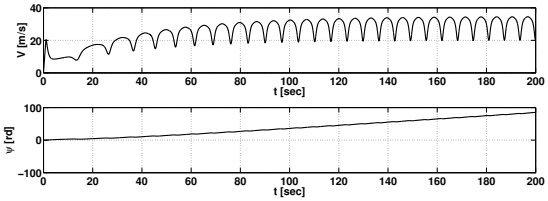

Fig. 5. (top) Car-like mobile robot velocity V, (bottom) car-like mobile robot yaw ψ.

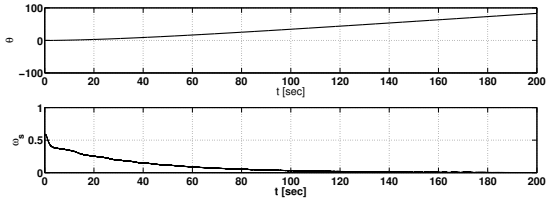

Fig. 6. (top) Path parameter θ, (bottom) speed assignment controller ω_s.

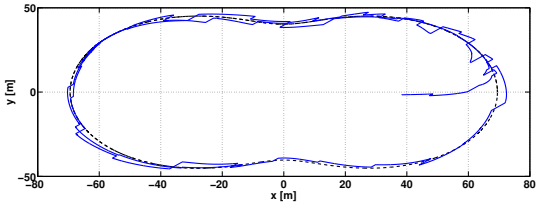

Fig. 7. Simulation results of the path following controller in the case of mobile robot localization errors. Desired path (dashed line), mobile robot path (continuous line)

where Δ_1 represents the approximately constant error, set as 10 m, and Δ_2 is a random error between $0 - 3$ m. Figure 7 shows the car-like mobile robot in the presence of localization errors. As it can be observed the path followed by the car-like mobile robot remains close to the desired path. This is very promising concerning experimental evaluation of the proposed controller as our available localization system has an error similar to the error modeled in equation (17).

Figure 8 shows the time histories of the path following errors as it can be observed the proposed controller is not able to drive it to zero, however the path errors have a bounded behavior as predicted by the theory.

Figure 9 shows the time histories of the control inputs while Figure 10 shows the behavior of the car–like velocity and yaw angle.

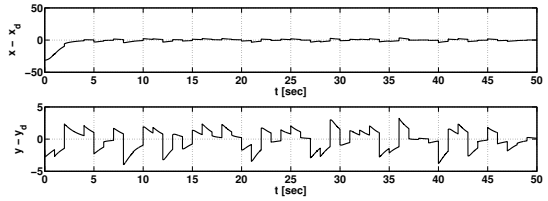

Fig. 8. Path following errors. (top) $x - x_d(\theta)$, (bottom) $y - y_d(\theta)$.

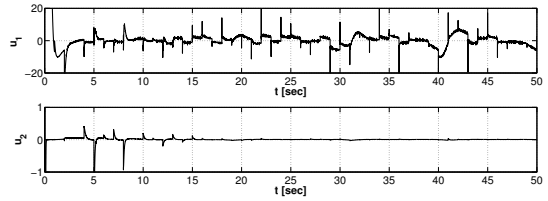

Fig. 9. Control signals. (top) u_1, (bottom) u_2.

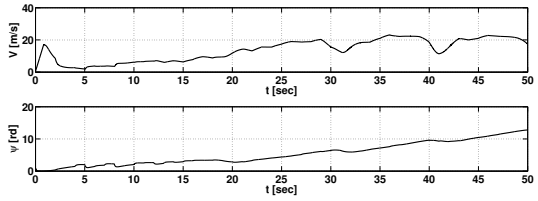

Fig. 10. (top) Car-like mobile robot velocity V, (bottom) car-like mobile robot yaw ψ.

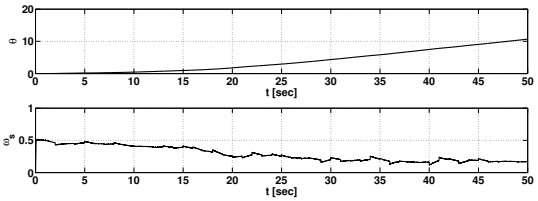

Fig. 11. (top) Path parameter θ, (bottom) speed assignment controller ω_s.

Finally, we show the time histories of the parameter of the path and the speed assignment controller. As it can be observed, the virtual controller ω_s does not converge to zero but remains bounded.

V. Conclusion

The problem of path following for the car–like mobile robot has been addressed and solved by means of a nonlinear controller based on input–output feedback linearization and the output maneuvering control approach introduced in [1]. We have analyzed the proposed controller in two scenarios, the first one assumes that the car–like mobile robot position is accurately measured or estimated and the second case considers that there is an error in the car–like mobile robot localization system. As expected, the performance of the proposed controller is degraded due to the errors in the localization system however it keeps all signals bounded. Numerical simulations have been used to illustrate the properties of the closed–loop system.

Some issues are left open in this work. First, the computation of the ultimate state bounds and a possible modification of the proposed controller to have a positive effect on these bounds. Second, the experimental test of the proposed controller and the inclusion of skidding and slipping effects.

References

[1] T. I. Fossen R. Skjetne and P. Kokotovic. Robust output maneuvering for a class of nonlinear systems. *Automatica*, 40:373–383, 2004.

[2] J. Borenstein, H. R. Everett, L. Feng, and D. Wehe. Mobile robot positioning- sensors and techniques. *Journal of Robotic Systems, Special Issue on Mobile Robots*, 14:231–249, 1997.

[3] T. W. McLain D. R. Nelson, D. B. Barber and R. W. Beard. Vector field path following for miniature air vehicles. *IEEE Trans. on Robotics*, 23:519–529, 2007.

[4] C.Samson. Control of chained systems application to path following and time-varying point-stabilization of mobile robots. *IEEE Transactions on Automatic Control*, 40(1):64–67, 2003.

[5] Z. Jiang and H. Nijmeijer. Tracking control of mobile robots: a case study in backstepping. *Automatica*, 33(7):1393–1399, 1997.

[6] C. Altafini. Path following with reduced off-tracking for multibody wheeled vehicles. *IEEE Transaction on Control Systems Technology*, 11(4):598–605, 2003.

[7] D. Soetanto, L. Lapierre, and A. Pascoal. Adaptive, non-singular path-following control of dynamic wheeled robots. In *Proceedings of the IEEE Conference on Decision and Control*, pages 1765–1770, Maui, Hawaii USA, 2003.

[8] J. O. Hespanha A. P. Aguiar. Trajectory-tracking and path-following of underactuated autonomous vehicles with parametric modeling uncertainty. *IEEE Trans. on Automatic Control*, 52:1362–1378, 2007.

[9] D. Wang and C. B. Low. Modeling and analysis of skidding and slipping in wheeled mobile robots: Control design perspective. *IEEE Trans. on Robotics*, 23:676–687, 2008.

[10] C. B. Low and D. Wang. Gps-based path following for a car-like wheeled mobile robot with skidding and slipping. *IEEE Trans. on Control Systems Technology*, 16:340–347, 2008.

[11] R. W. beard E. P. Anderson and T. W. McLain. Real-time dynamic trajectory smoothing for unmanned air vehicles. *IEEE Trans. on Control Systems technology*, 13:471–477, 2002.

[12] C. G. Lo Bianco A. Piazzi and M. Romano. η^3-splines for the smooth path generation of wheeled mobile robots. *IEEE Trans. on Robotics*, pages 1089–1095, 2007.

[13] G. Ambrosino, M. Ariola, U. Ciniglio, F. Corraro, E. De Lellis, and Pironti. Path generation and tracking in 3-d for uavs. *IEEE Trans. on Control Systems Technology*, pages 980–988, 2009.

[14] J. D. Lawrence. *A Catalog of Special Plane Curves*. Dover Publications, New York, 1972.

[15] B. D'Andrea-Novel, G. Bastin, and G. Campion. Dynamic feedback linearization of nonholonomic wheeled mobile robots. In *Proceedings of the IEEE International Conference on Robotic and Automation*, pages 2527–2532, Nice, France, 1992.

[16] G. Oriolo, A. De Luca, and M. Venditteli. Wmr control via dynamic feedback linearization: Design, implementation, and experimental validation. *IEEE Transaction on Control Systems Technology*, 10(6):835–852, 2002.

[17] R. Orosco, E. Aranda, and M. Velasco. Modeling and dynamic feedback linearization of a multi-steered n-trailer. In *Proceedings of the 15th IFAC World Congress*, Barcelona, Spain, 2002.

[18] G. Campion, G. Bastin, and B. D'Andréa-Novel. Structural properties and classification of kinematics and dynamics models of wheeled mobile robots. *IEEE Transactions on Robotics and Automation*, 12(1):47–61, 1996.

[19] G. Campion and W. Chung. *Springer Handbook of Robotics*, chapter 17. Wheeled Robots, pages 391–410. Springer, Berlin, Heidelberg, 2008.

[20] A. Isidori. *Nonlinear Control Systems*. Springer-Verlag, New York, 1995.

[21] H. K. Khalil. *Nonlinear Systems, Third Edition*. Prentice Hall, 2002.